NUCLEAR CHARGE AND MASS YIELDS FOR $^{235}U(n_{th},f)$

H.-G. Clerc, W. Lang, H. Wohlfarth, K.-H. Schmidt*
Institut für Kernphysik, Technische Hochschule Darmstadt, W. Germany

H. Schrader, The Lohengrin Collaboration,
Institut Laue-Langevin, Grenoble, France

Abstract

The fission product mass spectrometer "Lohengrin" has been used to determine the mass and nuclear charge yields of light fission products as a function of their kinetic energy in the range 88.5 MeV $\leq$ E $\leq$ 112.0 MeV. The proton pairing causes fine structures in the yields even at low kinetic energy. The large relative yields of nuclei with N $\geq$ 60 at high kinetic energy are tentatively explained by an oblate deformation of these nuclei at the scission point.

1. Introduction

The nuclear charge and mass distribution at different fission product kinetic energies may give important information about the fission process. By varying the kinetic energy, the total excitation energy of the two fragments may be varied. The total excitation energy is given by the collective excitation at scission (including the deformation energy of the fragments) and by the intrinsic excitation energy at scission. Particularly in the case of thermal-neutron-induced fission of ^{235}U, a fixed kinetic energy of the light fission products corresponds to a total excitation energy which is almost independent of the mass split. Measurements at low kinetic energy corresponding to high excitation energy may indicate to what extent the system is heated up during its motion from saddle to scission. As a consequence, the pairing correlations would be destroyed and as a result, the fine structure in the nuclear charge and mass distribution would disappear. On the other hand, measurements at very high kinetic energies permit fragments of very low excitation energy to be produced. Experimentally the total excitation energy of the two fragments can be reduced to a few MeV. Neutron emission is then no longer possible, and the mass distribution of the original fragments can be measured directly. Particular attention is drawn to the fact that in this case the fragments are formed with energies being only slightly larger than their ground state energies. It may therefore be assumed that the ground state nuclear structure of the fragments, e.g. the ground state deformation, has an important influence on the fission process.

In the following, measurements of the nuclear charge and mass distribution will be reported in which the kinetic energy of the light fission products has been varied between 88.5 and 112.0 MeV. This corresponds to a total fragment excitation energy of about 44 to 5 MeV. Measurements of the nuclear charge distribution at medium kinetic energies have been described previously[1,2].

2. Experimental set-up

The measurements were performed at the mass spectrometer "Lohengrin"[3] of the Institut Laue-Langevin in Grenoble. The fission product source had a thickness of about 40 µg/cm² UO_2 (93% ^{235}U). Due to the energy loss of the fission products in the source, their initial kinetic energy was smeared out by less than 1 MeV. Thus the kinetic energy was sufficiently well defined for the purpose of the present measurements. The size of the source and the exit slit at "Lohengrin" were chosen to obtain a mass resolving power $A/\Delta A$ = 400 (full-width $\frac{1}{10}$ maximum).

In order to measure mass spectra at specific ionic charge values, the fission products were detected with a silicon surface barrier detector at the exit slit of the spectrometer[4]. The nuclear charge distribution for a given mass number A and ionic charge state q was determined by measuring the fission product energy loss in a homogeneous carbon absorber[5] by a time-of-flight technique[6] as described previously[7]. As an example, fig. 1 shows time-of-flight spectra behind the carbon absorber for the isobar A = 96 at different initial kinetic energies. The Z resolution was in all cases sufficient to separate neighbouring elements. In order to determine the intensities of the lines corresponding to different elements, the spectra were unfolded by a computer program[2]. Fig. 1 demonstrates the influence of the neutron evaporation process on the nuclear charge distribution: The fission products at low kinetic energies are the residues of highly excited primary fission fragments which have evaporated several neutrons. Therefore the

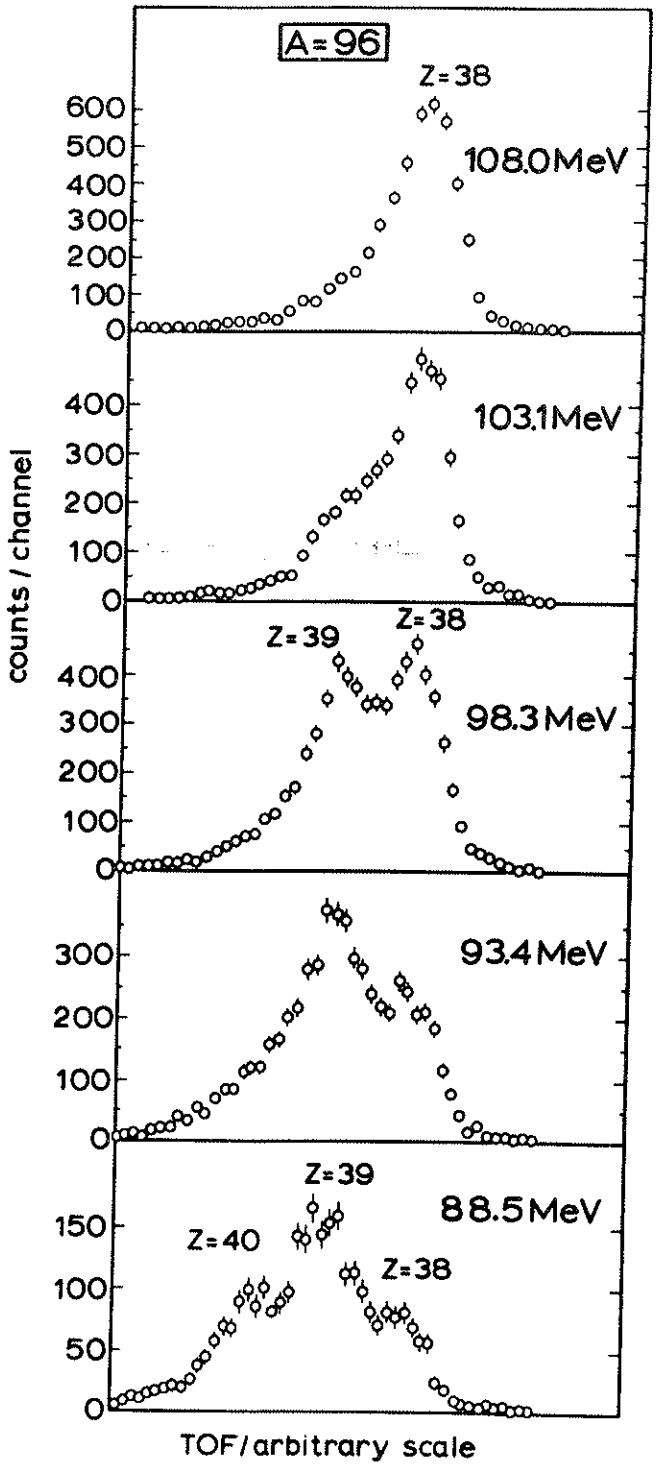

Fig. 1 Time-of-flight spectra behind the carbon absorber for fission products with mass number A = 96 at different initial kinetic energies

average nuclear charge increases with decreasing kinetic energy.

3. Results

3.1 Ionic charge state distributions

The ionic charge state distributions at a given mass number A were determined for the light fission products at 88.5 and 98.3 MeV kinetic energy. As an example, fig. 2 shows ionic charge state distributions for A = 88 and A = 89. An increased width and a shift to higher q-values for A = 89 when compared to A = 88 is clearly visible. Fig. 3 shows the average ionic

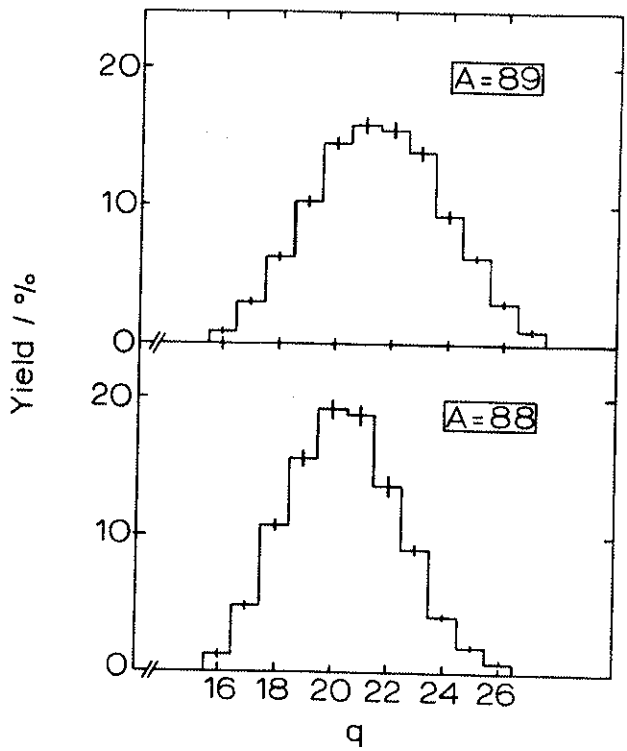

Fig. 2 Ionic charge state distributions of fission products with A = 88 and A = 89 at 98.3 MeV kinetic energy

charge state $\bar{q}$ and the square root of the second moment σ_q of the ionic charge distributions as a function of A at a kinetic energy of 98.3 MeV. The fine structure is caused by an increased width σ_q and an simultaneous increase in $\bar{q}$ for some mass numbers, particularly for A = 86, 89, 92 and 99. This is most probably caused by the internal conversion of some excited nuclear states of specific isotopes. If the lifetime of these excited states exceeds 10^{-14} s they will decay behind the fission source layer. The Auger cascade following the internal conversion process then leads to an increased ionic charge for these isotopes in the mass spectrometer.

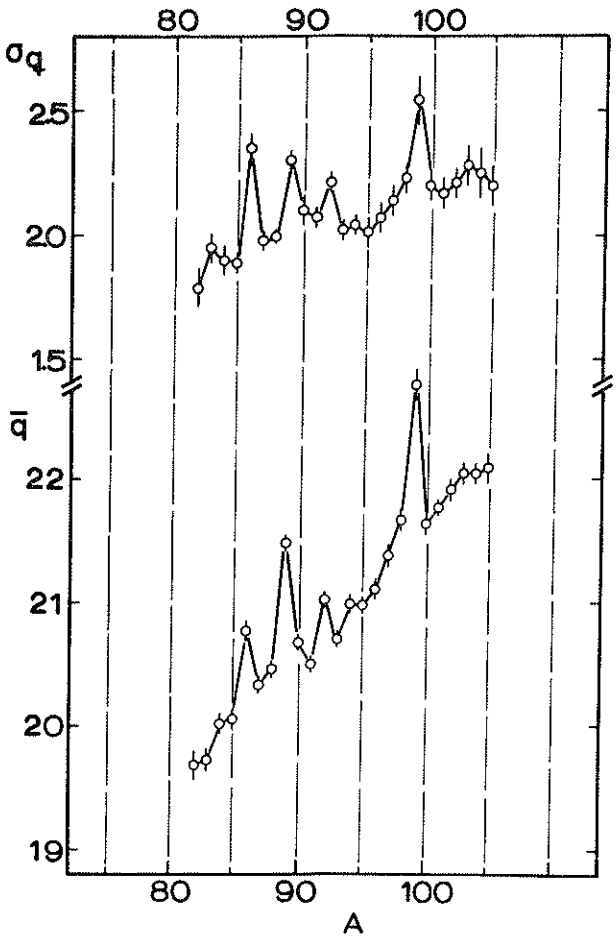

Fig. 3 Average ionic charge state $\bar{q}$ and square root of the second moment σ_q of the ionic charge state distribution as a function of the fission product mass number A for 98.3 MeV kinetic energy

3.2 Mass distributions, nuclear charge distributions, isotopic yields and element yields

The mass distributions at 88.5 and 98.3 MeV were obtained by summing up the contributions of the different ionic charge states to each mass number. At 108.0 and 112.0 MeV the mass distributions were measured only at q = 21. The resulting mass distributions at the various kinetic energies are shown in fig. 4.

For the nuclear charge distribution measurements, the ionic charge states q were selected to be within one unit of the average ionic charge state in almost all cases. The selected ionic charge states were in the interval $20 \leq q \leq 22$ (see table 1 and 2 and ref.[2]). The nuclear charge yields for kinetic energies close to the most probable kinetic energy published recently[2] were slightly extrapolated to a kinetic energy of 98.3 MeV so that they may be used together with the present mass yield measurements at 98.3 MeV. In

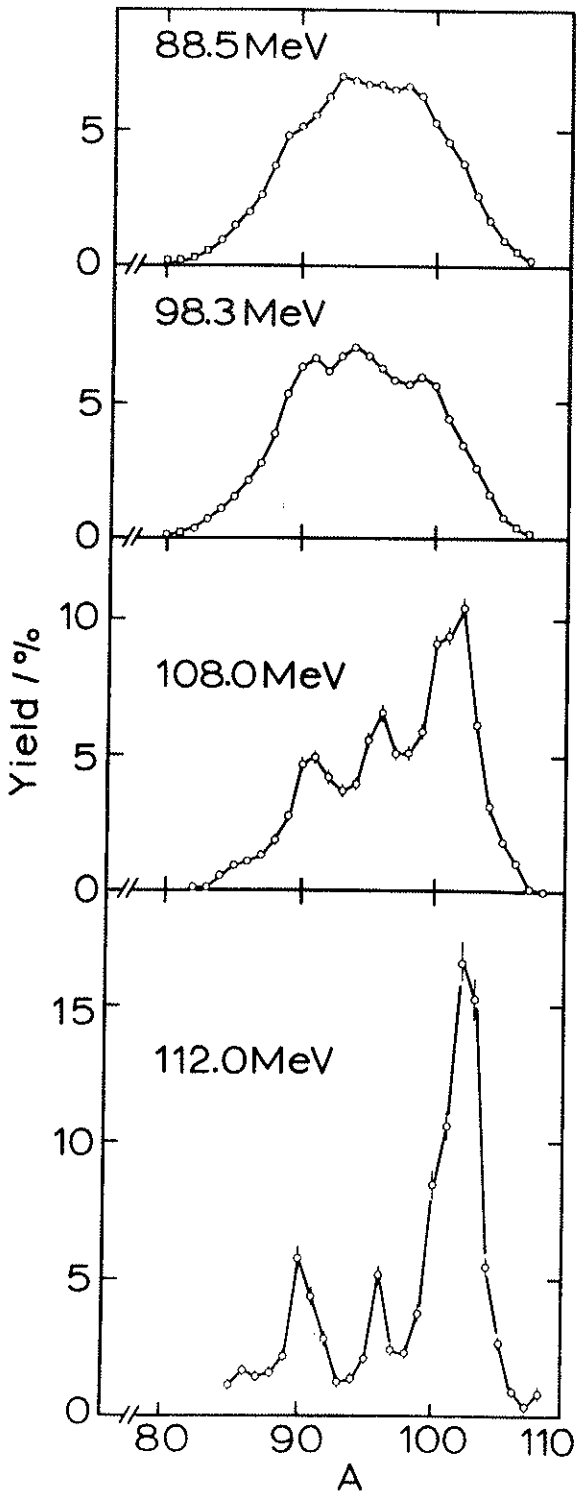

Fig. 4 Mass distributions for the light fission products from $^{235}U(n_{th},f)$ at different fission product kinetic energies. The distributions at 88.5 MeV and 98.3 MeV were obtained by summing up the contributions of all ionic charge states to a specific mass number A, while the distributions at 108.0 MeV and 112.0 MeV correspond to the ionic charge state q = 21

table 1 new results obtained at 108.0 MeV are presented, part of which were discussed recently[8]. Table 2 gives results for some mass numbers at very high kinetic energies close to 112 MeV. The analysis of the measurements at other kinetic energies has not yet been completed.

In order to calculate isotopic distributions from the Z-yields, the mass distributions measured at the same kinetic energy for the ionic charge state q = 21 were used. For this reason the isotopic distributions shown in fig. 5 correspond to measurements close to the average ionic charge state $\bar{q}$. From our knowledge of the ionic charge distributions it can be expected that the yields shown in fig. 5 are in most cases close to the yields integrated over all ionic charge states. Only the yields of a small number of nuclei, particularly the yield for at least one nucleus in each of the mass chains A = 86, 89, 92 and 99, will probably have to be corrected noticeably when the recently measured Z-yields for all ionic charges states will be available.

Fig. 6 shows the element yields as obtained by summing over the isotopic yields in fig. 5.

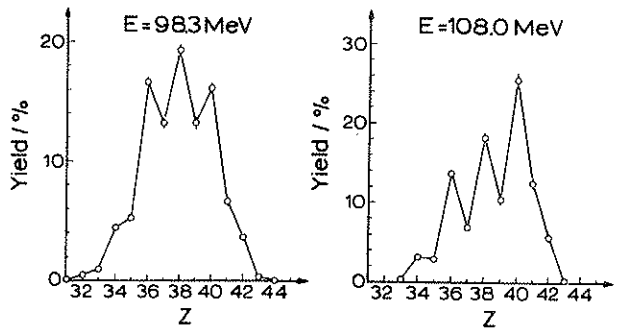

Fig. 6 Element yield distributions for the light fission products at 98.3 MeV and 108.0 MeV kinetic energy

4. Discussion

4.1 Odd-even effect

Fig. 7 shows the width parameter σ of the isobaric nuclear charge distributions plotted as a function of the mean nuclear charge $\bar{Z}$ for 98.3 and 108.0 MeV. In addition results are shown for other kinetic energies in a restricted mass range ($89 \leq A \leq 96$). The width parameter is seen to oscillate regularly as a function of $\bar{Z}$. This effect was previously found for energy-averaged yields[9] as well as for the yields at the most probable kinetic energy[2], and was shown to be mainly due to the proton pairing effect. If the mean nuclear charge number is even, there will be two odd Z's on either side which are strongly suppressed thus resulting in a small distribution width. On the other hand, a broad distribution will be obtained if the mean Z-values is odd and the two even charges on both sides are enhanced by the pairing effect. A certain influence of the neutron odd-even effect, particularly at high kinetic energies, is also observed. An important result seems to be that the proton pairing effect is quite strong at kinetic energies far below the most probable values, too. This conclusion is supported by the fine structure in the low energy mass distribution to be discussed below. The partial preservation of proton pairing in this case is much more exciting than in the high kinetic energy events where only a few MeV of excitation energy are available. This may be explained by the assumption[10] that the low kinetic energy events correspond to particularly elongated shapes at scission so that most of the energy is bound in fragment deformation energy.

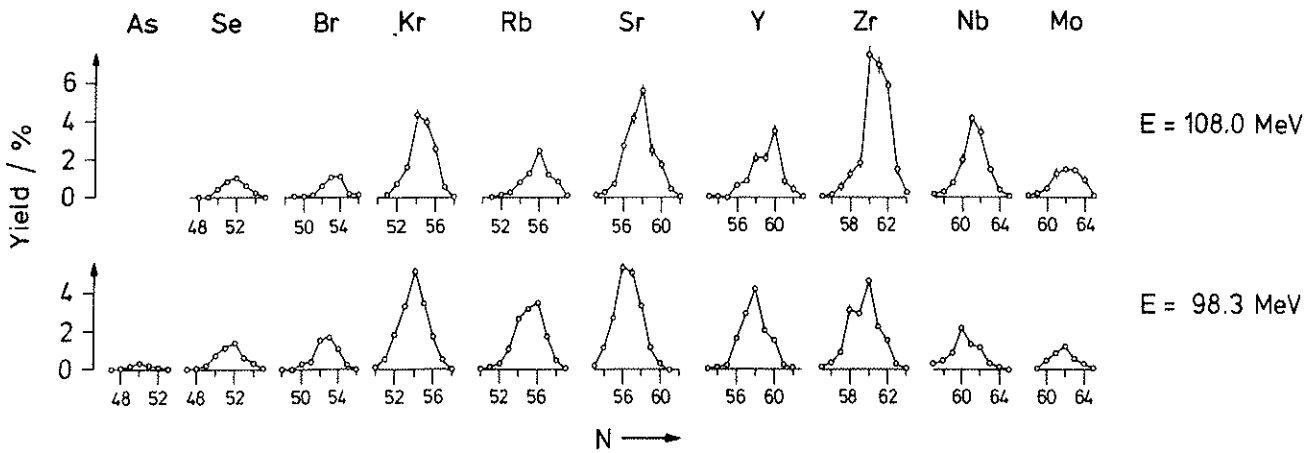

Fig. 5 Isotopic yield distributions for the light fission products at 98.3 MeV and 108.0 MeV kinetic energy

Table 1. Independent yields (%) and the nuclear charge distribution parameters $\overline{Z}$ and σ at a kinetic energy of 108.0 MeV .

A/q	Z = 33	34	35	36	37	38	39	40	41	42	43	$\overline{Z}$	σ
84/20	20.5±1.5	75.5±3.0	4.0±2.3									33.84±.03	.47±.03
85/20	6.3±1.6	92.1±3.4	1.6±1.6									33.95±.03	.28±.04
86/20		91.1±2.7	8.9±2.6									34.09±.03	.29±.04
87/20		47.3±3.0	44.0±3.2	8.7±1.8								34.61±.04	.64±.02
88/20		11.1±1.5	52.1±2.0	35.2±1.7	1.6±1.3							35.27±.04	.67±.03
89/21		.5± .5	37.8±2.1	57.2±3.1	4.5±2.2							35.66±.04	.57±.03
90/21			3.0± .7	92.5±5.3	4.5±2.7							36.02±.03	.27±.05
91/21			2.4± .8	79.1±4.5	16.0±3.6	2.5±1.3						36.19±.04	.50±.05
92/21				61.3±3.4	30.3±2.6	6.3±2.0	2.1±1.7					36.49±.06	.71±.07
93/20				13.9±1.9	65.6±3.2	19.2±3.4	1.3±1.3					37.08±.05	.61±.04
94/20				1.9± .7	29.1±1.8	69.0±3.1						37.67±.02	.51±.02
95/22					14.5±1.5	73.4±3.5	11.1±2.0	1.0±1.0				37.99±.03	.54±.04
96/22					1.4± .6	84.4±2.5	12.7±1.5	1.5±1.0				38.14±.03	.43±.04
97/21						48.9±4.5	40.8±4.5	10.3±4.0				38.61±.06	.67±.05
98/21						34.4±3.5	40.0±4.5	23.4±4.0	2.2±2.0			38.93±.07	.81±.05
99/21						5.0±1.5	54.5±2.5	38.0±2.0	2.5±1.5			39.38±.04	.62±.03
100/21						.6± .6	9.4±2.0	81.2±3.5	8.2±2.0	.6± .6		39.99±.03	.47±.04
101/22							4.5±2.0	73.2±4.0	20.8±2.5	1.5±1.2		40.19±.04	.53±.04
102/22								55.3±2.1	39.3±2.0	4.5±1.7	.9± .8	40.51±.04	.63±.05
103/22								24.1±4.5	55.9±4.5	20.0±4.5		40.96±.06	.66±.03
104/22								7.5±1.3	45.8±2.9	46.7±3.2		41.39±.03	.62±.02
105/22									20.8±3.0	77.0±4.5	2.2±2.2	41.81±.04	.44±.04

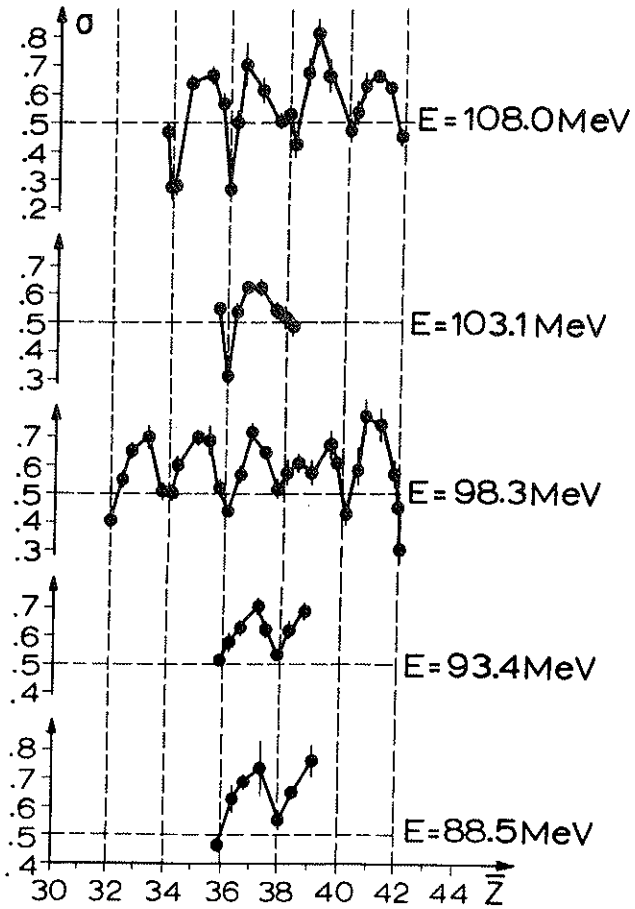

Fig. 7 Isobaric nuclear charge distribution width parameter σ as a function of the mean nuclear charge $\bar{Z}$ for different kinetic energies

All mass distributions shown in fig. 4 exhibit fine structure being more pronounced at the higher kinetic energies. In addition to this, the mass distribution becomes strongly asymmetric at high kinetic energies with an absolute maximum at the mass numbers A = 102 and A = 103. Below A = 100, the fine structure can be correlated with the odd-even proton effect: Even nuclear charge numbers dominate in the fine structure maxima, while odd nuclear charge numbers predominate in the minima. Due to neutron evaporation, the maxima are shifted towards smaller A-values when the kinetic energy is decreased.

The isotopic yield distributions (fig. 5) as well as the element distributions (fig. 6) clearly demonstrate the preferential formation of even-Z elements. In order to obtain a quantitative measure of the odd-even proton effect, the ratio of the summed yields of even-Z elements to the average summed yields $2\sum_e/(\sum_e + \sum_o)$ can be calculated. Thus an effect of (21±1)% for 98.3 MeV and (33±2)% for 108.0 MeV is obtained.

Fig. 5 reveals a distinct odd-even effect also for neutrons which is however much smaller than in the proton case. Due to neutron evaporation, the contribution of the fission process itself to the observed effect is difficult to assess.

4.2 The influence of shell effects at high kinetic energies

We now turn to a discussion of the enhancement of masses near A = 102 in the high energy mass distributions. A similar effect was found previously by Fraser et al.[11] and Reisdorf et al.[12]. This enhancement cannot be explained by the odd-even proton effect. A comparison of the isotopic distributions (fig. 5) or the Z-distributions (fig. 6) at 98.3 and 108.0 MeV reveals that the relative yield of Nb (Z = 41) is about a factor of two larger at 108.0 MeV than at 98.3 MeV, while all other odd-Z yields at 108.0 MeV are smaller than at 98.3 MeV. If looked at more closely, fig. 5 shows furthermore that the relative yield of almost all nuclei with N ≥ 60 is larger at 108.0 MeV than at 98.3 MeV.

At 112 MeV, the mass numbers A = 102 and A = 103 have the largest yields which is mainly due to the nuclei $^{102}_{40}Zr^{62}$ and $^{103}_{41}Nb^{62}$ (see table 2). Since neutron evaporation can be excluded at this high kinetic energy, the observed fission products are identical with the original fission fragments. Thus it seems that at high kinetic energies a division into a pair of fragments with 62 and 82 neutrons is preferred.

In the thermal-neutron induced fission of ^{233}U no enhancement of fragments near A = 102 at high kinetic energies was found[12]. This may be explained by the fact that in the fissioning system ^{234}U with two neutrons less than ^{236}U, N = 62 and 82 cannot be attained simultaneously.

In fig. 8 the total excitation energy of the two fragments as calculated from recent mass tables[13] is plotted for a kinetic energy of the light fragment of 112.0 MeV. For even A-values, the Q-value for even-even fragments was taken, and for odd A-values the larger of the two Q-values for even-odd and odd-even fragments was taken. Fig. 8 shows that the asymmetric mass distribution at 112.0 MeV is not caused by the Q-value, since E^*_{tot} decreases with increasing light fragment mass. In the mass region near A = 102, the total excitation energy of the two fragments is only about 5 MeV.

For the ground states of the nuclei in this Z-region, a large oblate deformation (β ≈ 0.3) was predicted[14,15] for the nuclei with N ≥ 60. Experimentally

Table 2. Independent yields (%) and the nuclear charge distribution parameters $\overline{Z}$ and σ at very high kinetic energies

A/q	E/MeV	Z = 40	41	42	$\overline{Z}$	σ
102/22	> 113	87.0±2.2	13.0±1.3		40.13±.02	.34±.02
103/22	> 113	9.5±1.1	81.6±3.0	8.9±2.4	40.99±.03	.43±.03
104/22	110	2.5±1.3	41.3±2.3	56.2±2.8	41.54±.03	.55±.03

a sudden onset of deformation was found from the energy of the first 2^+ state in the even-A isotopes of Sr, Zr and Mo when increasing the neutron number from 58 to 60 [16]. Since the excitation energy of the fragments is of the same magnitude as the shell correction leading to the deformed shape, the deformation of the ground state may be of decisive importance for the fission process at high kinetic energy. It seems possible that the scission configuration has a very compact shape consisting of a stiff spherical heavy fragment and an oblately deformed light fragment. This configuration corresponds to a high Coulomb energy and consequently results in a high fission fragment kinetic energy. The absolute value of the observed kinetic energy is compatible with the scission shape found from Hartree-Fock calculations[15].

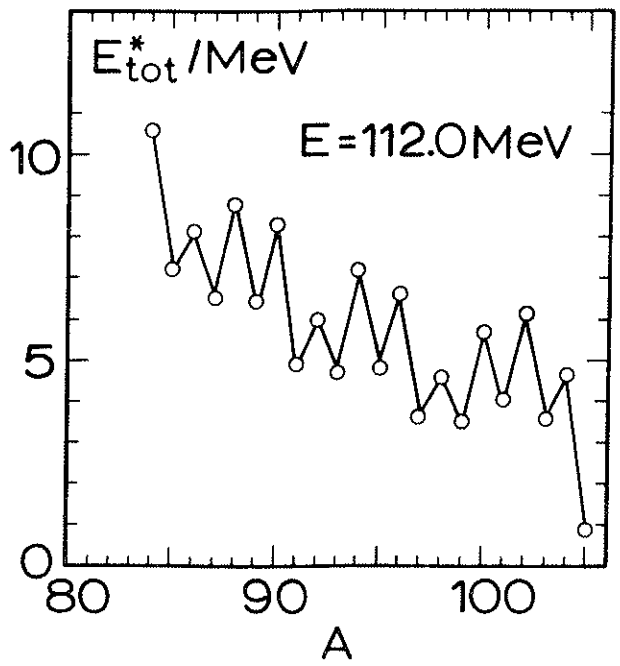

Fig. 8 Total excitation energy E^*_{tot} for the two fragments as a function of the light fission fragment mass number A at a fixed light fission fragment kinetic energy of 112.0 MeV. The mass tables of ref.[13] were used in the calculation.

In conclusion it may be stated that the $^{235}U(n_{th},f)$ yields are strongly influenced by the proton pairing effect at all kinetic energies. At high kinetic energies, the yield seems to be determined by shell effects for $N \geq 60$ and the complementary neutron shell at N = 82. The instability of the light fragments against oblate deformation for $N \geq 60$ may result in a particularly large relative yield of these nuclei at high kinetic energy.

The authors wish to acknowledge fruitful discussions with P. Armbruster and W.N. Reisdorf. - This work was supported in part by GSI Darmstadt.

References

1 H.-G. Clerc, K.-H. Schmidt, H. Wohlfarth, W. Lang, H. Schrader, K.E. Pferdekämper, R. Jungmann, M. Asghar, J.P. Bocquet, G. Siegert, Nucl. Phys. A 247, 74 (1975)

2 H.-G. Clerc, W. Lang, H. Wohlfarth, K.-H. Schmidt, H. Schrader, K.E. Pferdekämper, R. Jungmann, Z. Physik A 274, 203 (1975)

3 E. Moll, H. Schrader, G. Siegert, M. Asghar, J.P. Bocquet, G. Bailleul, J.P. Gautheron, J. Greif, G.I. Crawford, C. Chauvin, H. Ewald, H. Wollnik, P. Armbruster, G. Fiebig, H. Lawin, K. Sistemich, Nucl. Instrum. Methods 123, 615 (1975)

4 H. Wohlfarth, W. Lang, H.-G. Clerc, H. Schrader, K.-H. Schmidt, H. Dann, to be published

5 H. Wohlfarth, K.-H. Schmidt, H.-G. Clerc, H. Wirth, G. Lang, annual report 1974 of the Max-Planck-Institut für Kernphysik Heidelberg, p. 140

6 W. Lang, H.-G. Clerc, Nucl. Instrum. Methods 126, 535 (1975)

7 H.-G. Clerc, K.-H. Schmidt, H. Wohlfarth, W. Lang, H. Schrader, K.E. Pferdekämper, R. Jungmann, M. Asghar, J.P. Bocquet, G. Siegert, Nucl. Instrum. Methods 124, 607 (1975)

8 W. Lang, H.-G. Clerc, H. Wohlfarth, K.-H. Schmidt, H. Schrader, in Proceedings of the International Workshop IV on: Gross Properties of Nuclei and

Nuclear Excitations, Hirschegg, 1976, AED-Conf-76-015-000 (Darmstadt IKD, 1976), p. 147

9 G. Siegert, J. Greif, H. Wollnik, G. Fiedler, R. Decker, M. Asghar, G. Bailleul, J.P. Bocquet, J.P. Gautheron, H. Schrader, P. Armbruster, H. Ewald, Phys. Rev. Lett. 34, 1036 (1975)

10 H. Nifenecker, C. Signarbieux, R. Babinet, J. Poitou, Proc. of the Third IAEA Symposium on the Physics and Chemistry of Fission, Rochester, New York, August 1973, Vol. II, p. 117

11 J.S. Fraser, J.C.D. Milton, H.R. Bowman, S.G. Thompson, Can. J. Phys. 41, 2080 (1963)

12 W.N. Reisdorf, J.P. Unik, L.E. Glendenin, Nucl. Phys. A 205, 348 (1973)

13 S. Liran, N. Zeldes, report IKDA 75/14, Institut für Kernpyhsik, Technische Hochschule Darmstadt (1975)

14 D.A. Arseniev, A. Sobiczewski, V.G. Soloviev, Nucl. Phys. A 139, 269 (1969)

15 D. Kolb, private communication

16 T.A. Khan, F. Horsch, in: Proceed. 3rd IAEA Symposium on Physics and Chemistry of Fission, Rochester 1973, Vol. II, p. 257, Vienna: 1974

*GSI, Darmstadt